Behavioral/Systems/Cognitive

Inhibitory Dendrite Dynamics as a General Feature of the Adult Cortical Microcircuit

Jerry L. Chen,[1,2] **Genevieve H. Flanders,**[1] **Wei-Chung Allen Lee,**[1,3] **Walter C. Lin,**[1,4] **and Elly Nedivi**[1,2,3]

[1]Picower Institute for Learning and Memory and Departments of [2]Biology and [3]Brain and Cognitive Sciences, Massachusetts Institute of Technology, Cambridge, Massachusetts 02139, and [4]Harvard-MIT Division of Health Science and Technology, Harvard Medical School, Boston, Massachusetts 02115

The mammalian neocortex is functionally subdivided into architectonically distinct regions that process various types of information based on their source of afferent input. Yet, the modularity of neocortical organization in terms of cell type and intrinsic circuitry allows afferent drive to continuously reassign cortical map space. New aspects of cortical map plasticity include dynamic turnover of dendritic spines on pyramidal neurons and remodeling of interneuron dendritic arbors. While spine remodeling occurs in multiple cortical regions, it is not yet known whether interneuron dendrite remodeling is common across primary sensory and higher-level cortices. It is also unknown whether, like pyramidal dendrites, inhibitory dendrites respect functional domain boundaries. Given the importance of the inhibitory circuitry to adult cortical plasticity and the reorganization of cortical maps, we sought to address these questions by using two-photon microscopy to monitor interneuron dendritic arbors of *thy1*-GFP-S transgenic mice expressing GFP in neurons sparsely distributed across the superficial layers of the neocortex. We find that interneuron dendritic branch tip remodeling is a general feature of the adult cortical microcircuit, and that remodeling rates are similar across primary sensory regions of different modalities, but may differ in magnitude between primary sensory versus higher cortical areas. We also show that branch tip remodeling occurs in bursts and respects functional domain boundaries.

Introduction

A common theme of nervous-system architecture is a modular principle of design. This principle is exemplified in the adult neocortex, which is composed of repetitive, largely stereotyped columnar units extending perpendicular to the pial surface and running across cellular lamina II–VI (Mountcastle, 1997). These minicolumns contain all major cortical cell types interconnected in the vertical dimension suggesting they may function as a computational module in the mature cortex. While the significance of cortical columnar organization in terms of circuit function is still unclear (Horton and Adams, 2005; Douglas and Martin, 2007), anatomical variations on the same theme are recognizable across multiple afferent modalities, with borders delineated by columnar architecture. Common features of vertical organization such as cell number per radial traverse, intrinsic circuitry, and laminar organization of input and output projections are thought to be developmentally specified before afferent ingrowth and cortical regionalization (O'Leary et al., 1994).

Experiments suggest that neocortical columnar modules are similar enough across areas to be functionally subverted by afferent

drive. Embryonic visual cortex transplanted into the somatosensory area can assume somatosensory columnar features (Schlaggar and O'Leary, 1991), and the rewiring of retinal inputs to the developing auditory thalamus causes auditory cortex to be driven by visual activity and develop aspects of visual cortical organization (Sharma et al., 2000). Postnatally, day-to-day experience continues to shape cortical representations in animals throughout their life (Buonomano and Merzenich, 1998). Manipulations to the sensory periphery can shift the functional boundaries of cortical map representations, and the expansion or contraction of these maps has been shown to be accompanied by the repositioning of neuronal arbors to reflect new functional borders (Kossel et al., 1995; Hickmott and Steen, 2005).

Recently, chronic two-photon *in vivo* imaging has revealed aspects of experience-dependent structural remodeling that continues throughout life (Holtmaat and Svoboda, 2009). Formation and elimination of dendritic spines on excitatory pyramidal neurons have been shown across different cortical regions (Holtmaat et al., 2005; Zuo et al., 2005; Majewska et al., 2006), although due to experimental confounds related to varied image acquisition and analysis protocols, it has been unclear whether spine dynamics differ between cortical functional domains. Dendritic arbors of inhibitory interneurons have also been shown to remodel on a day-to-day basis in primary visual cortex (V1) (Lee et al., 2006), but it is unknown whether this is a general feature of cortical microcircuits across functional domains outside of V1. It is also unknown whether, like pyramidal dendrites, inhibitory dendrites respect functional domain boundaries. Given the importance of the inhibitory circuitry to adult cortical plasticity and the reorganization of cortical maps (Jacobs and Donoghue, 1991;

Jones, 1993), we sought to address these questions by monitoring inhibitory dendritic arbor dynamics in cells across multiple regions of adult mouse cortex.

Materials and Methods

Surgical procedure. To allow long-term visualization of *in vivo* neuronal morphology, cranial windows were implanted bilaterally over the visual cortices of adult male *thy1*-GFP-S mice (postnatal days 42–57) as previously described (Lee et al., 2008). Five-millimeter-diameter cranial windows were positioned with their medial edge directly apposing the midline and their anterior edge directly apposing bregma. Animals were housed singly for the remainder of the experiment. Sulfamethoxazole (1 mg/ml) and trimethoprim (0.2 mg/ml) were chronically administered in the drinking water through the final imaging session to maintain optical clarity of implanted windows.

Two-photon imaging. Starting at 3 weeks after cranial window surgery, adult male mice were anesthetized with 1.25% Avertin (7.5 ml/kg, i.p.). Anesthesia was monitored by breathing rate and foot pinch reflex, with additional doses administered as needed. *In vivo* two-photon imaging was performed using a custom-built microscope modified for *in vivo* imaging with a stereotaxic restraint affixed to a stage insert and custom acquisition software. The light source for two-photon excitation was a commercial Mai Tai HP Ti:Sapphire laser (Spectra-Physics) pumped by a 14 W solid state laser delivering 100 fs pulses at a rate of 80 MHz with the power delivered to the objective ranging from ~37 to 50 mW depending on imaging depth. Z-resolution was obtained with a piezo actuator positioning system (Piezosystem Jena) mounted to the objective. The excitation wavelength was set to 950 nm, with the excitation signal passing through a 20×/1.0 NA water-immersion objective (Plan-Apochromat, Zeiss) and collected after a barrier filter by a photomultiplier tube. Given the sparse GFP expression in the *thy1*-GFP-S line, typically only one cell was imaged per animal. While there has been some debate regarding an inflammatory response in the cranial window preparation affecting dendritic spine dynamics (Xu et al., 2007), we have previously shown that cranial window insertion and imaging by our protocol does not affect dendritic arbor or spine dynamics directly or through recruitment of an immune response (Lee et al., 2008).

Optical intrinsic signal imaging. For functional identification of monocular and binocular visual cortex, optical imaging of intrinsic signal and data analysis were performed as described previously (Kalatsky and Stryker, 2003). Mice were anesthetized and maintained on 0.5–0.8% isoflurane supplemented by chlorprothixene (10 mg/kg, i.m.), and placed in a stereotaxic frame with heart rate continuously monitored. For visual stimuli, a horizontal bar (5° in height and 73° in width) drifting up with a period of 12 s was presented for 60 cycles on a high-refresh-rate monitor positioned 25 cm in front of the animal. Optical images of visual cortex were acquired continuously under a 610 nm illumination with an intrinsic imaging system (LongDaq Imager 3001/C; Optical Imaging) and a 2.5×/0.075 NA (Zeiss) objective. Images were spatially binned by 4 × 4 pixels for analysis. Cortical intrinsic signal was obtained by extracting the Fourier component of light reflectance changes matched to the stimulus frequency whereby the magnitudes of response in these maps are fractional changes in reflectance. The magnitude maps were thresholded at 30% of peak response amplitude to define a response region. Primary visual cortex was determined by stimulation of both eyes. Binocular visual cortex was determined by stimulation of the ipsilateral eye. Monocular visual cortex was determined by subtracting the map of binocular visual cortex from the map of primary visual cortex.

Mapping of cell location. Stereotaxic coordinates for imaged cells were obtained through CCD camera images taken of the cell and the imaged window. Position along the anterior–posterior and medial–lateral axis was calculated by measuring the distance from the cell to the bregma and midline, respectively. In total, 14 of 15 V2 cells, 6 of 11 S1 cells, and 36 of 45 V1 cells were successfully mapped. The remaining cells were assigned to cortical region based on coarse position in the cranial window.

Data and statistical analysis. Using Matlab (MathWorks) and ImageJ (National Institutes of Health), 16 bit two-photon raw scanner data were converted into an 8 bit image *z*-stack. For each cell, 4-D (*x, y, z,* and *t*)

stacks were manually traced in Neurolucida (MicroBrightField) and analyzed blind to cortical area. Every imaged cell was independently reconstructed at each time point and branch tip length measurements were obtained for all branches. The only branch tips (segments of dendrite from the last branch point to the branch terminal ending) included in the analysis were those that could be confidently identified across all imaging sessions in relation to local landmarks, did not extend beyond the imaging volume, and were not obscured by blood vessels. New branches and branches eliminated in their entirety were included in the analysis. The branch length refers to the distance from the last branch point to the tip. For unbiased identification of dynamic branch tips, a Fano factor (FF) value was calculated based on branch tip length measurements obtained from Neurolucida across all imaging sessions. The FF is defined as the variance in the measured length of an individual branch tip across all imaging sessions, divided by the mean length of that branch tip [FF = $S^2/\bar{X}$, where $S^2 = [\Sigma(X - \bar{X})^2]/(n - 1)$]. The FF has been previously shown to represent the best nonbiased indicator of branch tip dynamics as compared to other methods of analysis and robustly identifies small branch tip changes while accounting for measurement variability during imaging or manual reconstructions (Lee et al., 2008). The reason that in practice the FF best represents the population of dynamic branch tips likely hinges on the fact that the majority of remodeling occurs on relatively short branch tips. Normalizing by the average branch tip length helps identify shorter branch tips that are dynamic and minimizes the effects of measurement variability/error in longer branch tips. A FF >1.09 for individual branch tips was empirically determined as the threshold between dynamic and stable branch tips scored by visual examination of all branch tips and corresponds to the 1.5 × interquartile FF range above the upper quartile of the entire population. Once branch tips were identified as having a FF > 1, their branch tip length measurement was included in the cell analysis. The mean FF across all monitored branch tips for each superficial L2/3 interneuron was calculated to confirm that each cell met the threshold (mean FF > 0.35) previously determined for a dynamic cell (Lee et al., 2008). In total, 1812 monitored dendritic branch tips of 2669 total branch tips from 71 cells from 71 animals were followed over 2–10 weekly imaging sessions. For each cell, rates of branch tip dynamics represent the fraction of dynamic branch tips out of the total branch tips monitored divided by the length of the entire imaging period. Branch tip bias index was determined from Neurolucida reconstructions where the dendritic field was bisected through the soma along a plane parallel to the nearest border. The number of branch tips extending into the hemifield located adjacent to versus remote to the border was quantified such that the bias index = (# branch tips away from border − # branch tips toward border)/(# branch tips away from border + # branch tips toward border). Wilcoxon rank sum test or Mann–Whitney *U* test was used for statistical analysis of time course data, where *n* indicates the number of cells. For length change per branch tip analysis, *n* indicates the number of branch tips. All error bars depict the SEM.

Results

To test whether interneuron remodeling is a cortical feature common to different primary as well as higher-level sensory regions, adult *thy1*-GFP-S transgenic mice expressing GFP in a random subset of neurons sparsely distributed within the superficial cortical layers were surgically implanted with 5 mm bilateral cranial windows. Windows were positioned lateral to the midline, between the bregma and lambda fissures, exposing primary visual (V1), secondary visual (V2), and primary somatosensory (S1) cortex. Following 3 weeks of recovery, superficial L2/3 interneurons (65–150 μm below the pial surface) were identified. Remodeling interneurons were previously shown to be restricted to superficial layer 2/3 (L2/3) (Lee et al., 2008), a laminar region that retains a considerable degree of plasticity in the adult (Gilbert and Wiesel, 1992; Diamond et al., 1994; Das and Gilbert, 1995; Rioult-Pedotti et al., 1998). The cortical location of each cell was mapped based on its stereotaxic coordinates (Fig. 1*D*). Two-
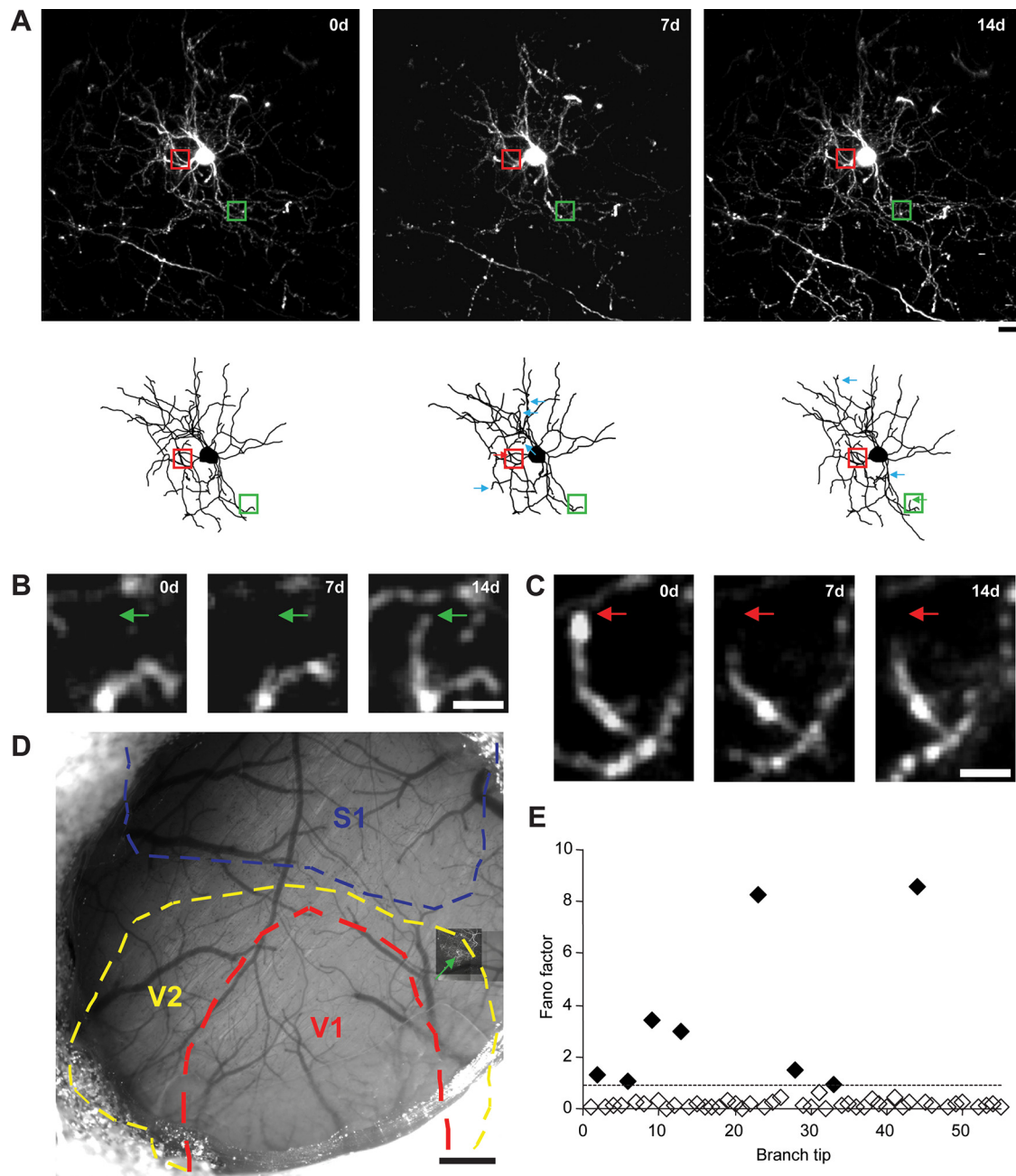
Figure 1. Chronic two-photon *in vivo* imaging of dendritic branch tip dynamics in superficial L2/3 cortical interneurons. ***A***, Maximum *z*-projection (MZP) near the cell body (above) along with two-dimensional projections of three-dimensional skeletal reconstructions (below) of a superficial L2/3 interneuron acquired over 2 weeks. Arrows indicate dynamic branch tips. ***B***, High-magnification view of one branch tip extension (green box and arrow in ***A***). Green arrow marks the approximate distal end of the branch tip at 14 d. ***C***, High-magnification view of one branch tip retraction (red box and arrow in ***A***). Red arrow marks the approximate distal end of the branch tip at 0 d. ***D***, MZP of chronically imaged interneuron (green arrow) superimposed over blood vessel map with primary visual cortex (V1, red), secondary visual cortex (V2, yellow), and primary somatosensory cortex (S1, blue) outlined. ***E***, Dynamic branch tip analysis of cell imaged in ***A***. Diamonds indicate Fano factor values of individual monitored branch tips with filled diamonds indicating dynamic branch tips. Dotted line marks the experimentally determined threshold for dynamic branch tip. Scale bars: ***A***, 200 μm; ***B***, 5 μm; ***C***, 0.5 mm.

photon imaging volumes encompassing the cell and all of its dendritic arbors were acquired at weekly intervals for a period of 2–10 weeks (Fig. 1*A*). Branch tips were reconstructed and monitored for length changes, which were then quantified using a Fano factor analysis (Fig. 1*B,C,E*).

We found that interneuron dendritic branch tips in adult S1, V1, and V2 all remodel on a week-to-week basis (Fig. 2*A*). Over several weeks of imaging, we routinely observed multiple dynamic branch tips per cell. This remodeling was not uniformly distributed across time; rather, it ranged from 0 to 9 tips per cell per week, with some weeks showing bursts of remodeling. With a

longer imaging protocol, one is more likely to "catch" these events of high dynamics, but their magnitude is less apparent when averaged with interleaving sessions of "nongrowth" (Fig. 2*B*). When averaged across weeks, comparison of branch tip remodeling in V1 and S1 showed similar dynamics, with 2.49 ± 0.33% and 2.52 ± 0.38% dynamic branch tips/week, respectively (Fig. 2*C*). V2 cells were significantly more dynamic than V1 and S1 cells at 4.28 ± 0.63% dynamic branch tips/week (V1 vs V2, Mann–Whitney *U* test, $p < 0.02$; S1 vs V2, Mann–Whitney *U* test, $p < 0.05$) (Fig. 2*C*). V2 cells were more likely to have a week where at least 8–9% of branch tips are dynamic (quite a rare event

in the other two groups) (V1 vs V2, Mann–Whitney U test, $p < 0.05$; S1 vs V2, Mann–Whitney U test, $p < 0.01$) (Fig. 2C). Interestingly, the fractional branch length change per cell and average length change per branch tip were not significantly different across cortical regions (data not shown). These data suggest that the higher baseline dynamics of V2 interneurons represents an increase in the number of dynamic branch tips per growth spurt as well as a higher frequency of growth spurts.

We next asked whether interneuron dendrite remodeling respects functional domain boundaries in a manner similar to excitatory dendrites. Whereas species such as cat, monkey, and ferret possess distinct eye-specific domains with sharp boundaries even on a local anatomical level (LeVay et al., 1978, 1980; Law et al., 1988), mouse visual cortex contains two general regions: a monocular zone (V1M), with inputs solely from the contralateral eye, and a binocular zone (V1B) with highly intermingled inputs from both eyes (Gordon and Stryker, 1996; Antonini et al., 1999). To assess whether dynamic interneuron branch tips respect the boundaries of these functional domains, we mapped the location of imaged cells relative to an area map of V1M and V1B which was generated from both optical intrinsic signal maps and coordinates from the Paxinos mouse brain atlas (Paxinos and Franklin, 2004) (Fig. 3 A, B). Based on the fact that the average radial extent for an interneuron dendritic field is 130 μm, we designated cells with soma <130 μm from the V1–V2 or V1M–V1B border as border cells, as they could potentially sample cross-border input if they are not radially biased. For each border cell, we analyzed the distribution of stable and dynamic branch tips relative to the nearest border by computing a branch tip bias index (Katz et al., 1989; Hübener and Bolz, 1992; Hickmott and Steen, 2005). The dendritic field was bisected through the soma along a plane parallel to the nearest border and the number of branch tips extending into the hemifields toward versus away from the border were compared (Fig. 3C). We found that stable branch tips of border cells were distributed with no clear bias toward or away from their nearest border (Fig. 3D). In contrast, dynamic branch tips were significantly biased away from the nearest border (border cells; stable branch tips versus dynamic branch tips, Mann–Whitney U test, $p < 0.005$). In nonborder cells, neither stable nor dynamic branch tips exhibited any border bias, suggesting that the border bias in branch tip remodeling is specific to cells located along functional boundaries.

Discussion

Using chronic *in vivo* monitoring of interneuron dendrites in different regions of the adult cortex, we find that interneuron branch tip remodeling occurs in primary visual and somatosensory cortices, as well as in higher-order visual cortex. Remodeling rates are similar in the V1 and S1 primary sensory regions, but are
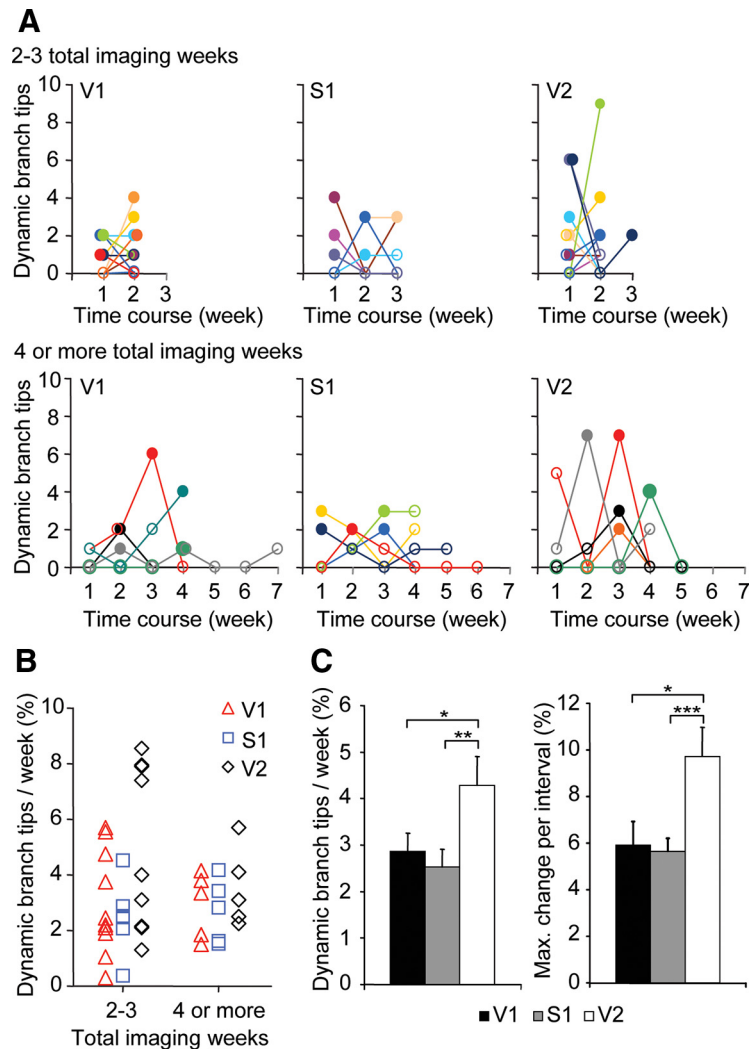

Figure 2. Interneuron dendritic branch tip dynamics across multiple cortical regions. **A**, Time course of dynamic branch tips by weekly imaging interval for individual cells in V1, S1, and V2. Filled points indicate maximal weekly branch tip change. Top panels represent cells imaged for 2 or 3 weeks. Bottom panels represent cells imaged for 4 or more weeks. **B**, Quantification of fractional rate of dynamic branch tips per week for individual cells in V1, S1, and V2. **C**, Comparison across cortical regions of fractional rate of dynamic branch tips (left) and maximal fractional branch tip change per week (right) (V1: n = 17 cells from 17 mice, 48 dynamic branch tips, 623 total branch tips; S1: n = 11 cells from 11 mice, 45 dynamic branch tips, 485 total branch tips; V2: n = 15 cells from 15 mice, 75 dynamic branch tips, 614 total branch tips) (***p < 0.01, **p < 0.02, *p < 0.05). Error bars, SEM.

significantly higher in V2 due to recruitment of more dynamic branch tips. We also find that remodeling branch tips respect functional domain boundaries. These findings indicate that interneuron dendrite remodeling is an intrinsic feature of the neocortical microcircuit.

Studies examining dendritic spine turnover on excitatory pyramidal neurons across cortical regions have shown that spine remodeling is also a common feature of the adult cortical microcircuit (Holtmaat et al., 2005; Zuo et al., 2005; Majewska et al., 2006). However, it has been unclear from these studies whether there are differences in dynamic rates across different cortical regions. The inconsistency in results has been attributed to sampling of different cell types, differences in imaging conditions, measurement variability, scoring methods, and cross-study comparisons between different groups. Without these potential confounds in our study, we find that within the specific population of superficial L2/3 interneurons monitored, cells in S1 and V1 exhibit no difference in rates of branch tip dynamics. Previous studies also show no difference in baseline
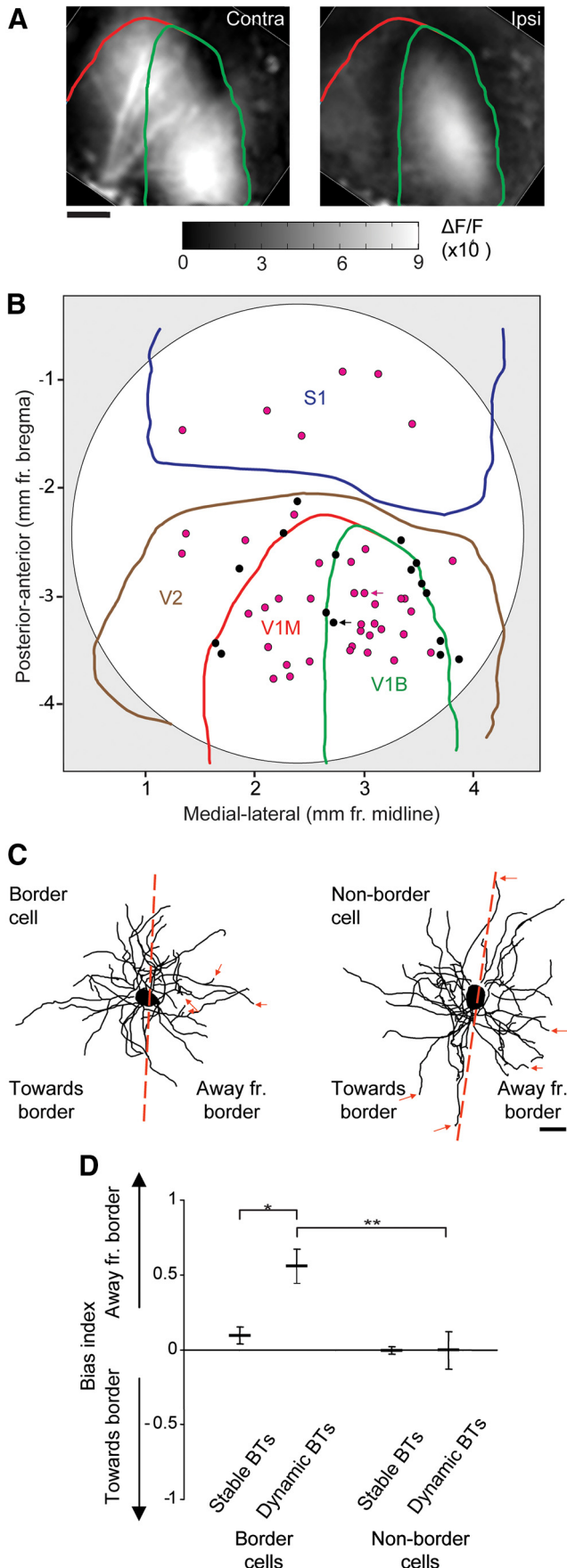
Figure 3. Dynamic branch tip bias in cells along functional cortical boundaries. **A**, Map of primary monocular (V1M) and binocular (V1B) visual cortex obtained by optical intrinsic signal

remodeling rates between monocular versus binocular visual cortex, although these areas respond differently to visual deprivation (Chen et al., 2011).

Cells within V2 exhibit higher dynamics compared to V1 and S1 due to a higher frequency of events and recruitment of more dendrites per event. Relatively little is known about the organization and function of V2 in rodent cortex. It is thought that mouse V2 is comprised of at least nine topographically distinct subregions (Wang and Burkhalter, 2007) and that there are fewer hierarchical levels found in rat than in cat or monkey (Coogan and Burkhalter, 1993). Mouse V2 receives feedforward input from V1 (Gonchar and Burkhalter, 2003; Dong et al., 2004a,b; Wang and Burkhalter, 2007) as well as reciprocal connections between subregions (Berezovskii et al., 2011). It also sends and receives input to and from other sensory systems (Wagor et al., 1980; Smith et al., 2010). A suggested purpose of spine and interneuron arbor remodeling is to increase access to distinct circuits within the local cortical volume (Stepanyants et al., 2002; Chen and Nedivi, 2010). Since the increased dynamics of V2 interneurons as compared to V1 and S1 is largely due to additional recruitment of remodeling dendrites, one can speculate that V2 neurons are more dynamic because they receive multiple distinct streams of input and may be required to locally adjust the relative weights of these inputs within the circuit. It will be interesting to determine whether enhanced remodeling is a feature unique to V2 or is a general feature of higher-order cortical areas.

In the feline and primate visual system, dendritic arbors of cortical neurons have been shown to respect the boundaries of ocular dominance columns (Katz et al., 1989; Kossel et al., 1995). Dendrites close to borders remain preferentially, although not exclusively, within their "home" column. When columnar boundaries were shifted in response to visual manipulations, dendrites did not remain within their original boundaries, but tended to cross more frequently into neighboring territory (Kossel et al., 1995). Dendritic bias has also been shown for neurons in rat somatosensory cortex that respect the functional boundary between the forepaw and lower jaw representations in S1 (Hickmott and Merzenich, 1999). This dendritic bias shifts in response to denervation reflecting the new location of the functional border (Hickmott and Steen, 2005). While the mouse visual cortex lacks ocular dominance columns, there is a functional boundary delineating the monocular and binocular zones and between primary and secondary visual areas (Gordon and Stryker, 1996). Our finding that the dynamic remodeling of inhibitory dendritic arbors respects these boundaries suggests that their functional relevance may relate to activity within their "home" region (the region containing the cell body). However, the lack of bias in the morphology of the stable arbor suggests that anatomical substrates also exist for interactions across boundaries.

←

imaging of contralateral (left) and ipsilateral (right) eye stimulation. Stereotaxic boundaries from the Franklin and Paxinos mouse brain atlas are overlaid in red (V1M) and green (V1B). **B**, Overlay of mapped imaged cells with cranial window (white region) and boundaries of respective cortical regions defined. Border cells (<130 μm from the nearest border) are denoted with black circles. Nonborder cells are denoted with magenta circles. **C**, Example of branch tip bias index calculation of a border cell (black arrow in **B**) and a nonborder cell (magenta arrow in **B**). Red dotted line indicates bisecting plane parallel to nearest boundary. Red arrows indicate dynamic branch tips. **D**, Quantification of branch tip bias for stable and dynamic branch tips in border and nonborder cells (border cells, $n = 16$; nonborder cells, $n = 37$) (**$p < 0.002$, *$p < 0.005$). Error bars, SEM.

The neocortex performs diverse sensory, motor, and cognitive tasks that are all strongly influenced by prior experience and can be modified through learning. Experience-dependent map plasticity and perceptual learning display many common features across sensory cortical areas (Feldman, 2009). The similarity of cellular plasticity mechanisms for the physiological modification of existing synapses as well as structural remodeling of cortical circuits in different modality cortices supports the concept of a common underlying infrastructure perhaps embodied in the modularity of neocortical microcolumns.

Inhibitory neurons play an important role in the cortical circuit, modulating the temporal response properties of excitatory neurons (Singer, 1996; McBain and Fisahn, 2001) and enhancing their ability to participate in spike timing-dependent plasticity (Dan and Poo, 2004; Foeller and Feldman, 2004). Inhibitory circuitry is crucial during development (Foeller and Feldman, 2004; Hensch, 2004) and has also been implicated in cortical map plasticity in the adult (Jacobs and Donoghue, 1991; Jones, 1993). Electrophysiological studies suggest that the potential site for reorganization of sensory and motor maps in the adult neocortex is in the horizontal projections of L2/3 (Singer, 1996; McBain and Fisahn, 2001), the idea being that map plasticity derives from unmasking of latent horizontal pathways regulated by local inhibitory neurons. Small adjustments in inhibitory tone could be sufficient to reweigh local connections and recalibrate cortical maps. We have previously shown that interneuron dendritic remodeling is specific to superficial layer 2/3 (Lee et al., 2008), where inhibition plays a critical role in adjusting map representations, and that this remodeling is driven by experience in an input- and circuit-specific manner (Chen et al., 2011). Here we show that interneuron dendritic branch tip remodeling is a general feature of the adult cortical microcircuit and that dynamics are sensitive to circuit context (V1 versus V2) and to location of functional boundaries. These findings together suggest that inhibitory dendrite remodeling may also be a common element of structural plasticity mechanisms built into the neocortical module.

References

Antonini A, Fagiolini M, Stryker MP (1999) Anatomical correlates of functional plasticity in mouse visual cortex. J Neurosci 19:4388–4406.

Berezovskii VK, Nassi JJ, Born RT (2011) Segregation of feedforward and feedback projections in mouse visual cortex. J Comp Neurol. Advance online publication. doi:10.1002/cne.22675.

Buonomano DV, Merzenich MM (1998) Cortical plasticity: from synapses to maps. Annu Rev Neurosci 21:149–186.

Chen JL, Nedivi E (2010) Neuronal structural remodeling: is it all about access? Curr Opin Neurobiol 20:557–562.

Chen JL, Lin WC, Cha JW, So PT, Kubota Y, Nedivi E (2011) Structural basis for the role of inhibition in facilitating adult brain plasticity. Nat Neurosci 14:587–594.

Coogan TA, Burkhalter A (1993) Hierarchical organization of areas in rat visual cortex. J Neurosci 13:3749–3772.

Dan Y, Poo MM (2004) Spike timing-dependent plasticity of neural circuits. Neuron 44:23–30.

Das A, Gilbert CD (1995) Long-range horizontal connections and their role in cortical reorganization revealed by optical recording of cat primary visual cortex. Nature 375:780–784.

Diamond ME, Huang W, Ebner FF (1994) Laminar comparison of somatosensory cortical plasticity. Science 265:1885–1888.

Dong H, Shao Z, Nerbonne JM, Burkhalter A (2004a) Differential depression of inhibitory synaptic responses in feedforward and feedback circuits between different areas of mouse visual cortex. J Comp Neurol 475:361–373.

Dong H, Wang Q, Valkova K, Gonchar Y, Burkhalter A (2004b) Experience-dependent development of feedforward and feedback circuits between lower and higher areas of mouse visual cortex. Vision Res 44:3389–3400.

Douglas RJ, Martin KA (2007) Mapping the matrix: the ways of neocortex. Neuron 56:226–238.

Feldman DE (2009) Synaptic mechanisms for plasticity in neocortex. Annu Rev Neurosci 32:33–55.

Foeller E, Feldman DE (2004) Synaptic basis for developmental plasticity in somatosensory cortex. Curr Opin Neurobiol 14:89–95.

Gilbert CD, Wiesel TN (1992) Receptive field dynamics in adult primary visual cortex. Nature 356:150–152.

Gonchar Y, Burkhalter A (2003) Distinct GABAergic targets of feedforward and feedback connections between lower and higher areas of rat visual cortex. J Neurosci 23:10904–10912.

Gordon JA, Stryker MP (1996) Experience-dependent plasticity of binocular responses in the primary visual cortex of the mouse. J Neurosci 16:3274–3286.

Hensch TK (2004) Critical period regulation. Annu Rev Neurosci 27:549–579.

Hickmott PW, Merzenich MM (1999) Dendritic bias of neurons in rat somatosensory cortex associated with a functional boundary. J Comp Neurol 409:385–399.

Hickmott PW, Steen PA (2005) Large-scale changes in dendritic structure during reorganization of adult somatosensory cortex. Nat Neurosci 8:140–142.

Holtmaat A, Svoboda K (2009) Experience-dependent structural synaptic plasticity in the mammalian brain. Nat Rev Neurosci 10:647–658.

Holtmaat AJ, Trachtenberg JT, Wilbrecht L, Shepherd GM, Zhang X, Knott GW, Svoboda K (2005) Transient and persistent dendritic spines in the neocortex in vivo. Neuron 45:279–291.

Horton JC, Adams DL (2005) The cortical column: a structure without a function. Philos Trans R Soc Lond B Biol Sci 360:837–862.

Hübener M, Bolz J (1992) Relationships between dendritic morphology and cytochrome oxidase compartments in monkey striate cortex. J Comp Neurol 324:67–80.

Jacobs KM, Donoghue JP (1991) Reshaping the cortical motor map by unmasking latent intracortical connections. Science 251:944–947.

Jones EG (1993) GABAergic neurons and their role in cortical plasticity in primates. Cereb Cortex 3:361–372.

Kalatsky VA, Stryker MP (2003) New paradigm for optical imaging: temporally encoded maps of intrinsic signal. Neuron 38:529–545.

Katz LC, Gilbert CD, Wiesel TN (1989) Local circuits and ocular dominance columns in monkey striate cortex. J Neurosci 9:1389–1399.

Kossel A, Löwel S, Bolz J (1995) Relationships between dendritic fields and functional architecture in striate cortex of normal and visually deprived cats. J Neurosci 15:3913–3926.

Law MI, Zahs KR, Stryker MP (1988) Organization of primary visual cortex (area 17) in the ferret. J Comp Neurol 278:157–180.

Lee WC, Huang H, Feng G, Sanes JR, Brown EN, So PT, Nedivi E (2006) Dynamic remodeling of dendritic arbors in GABAergic interneurons of adult visual cortex. PLoS Biol 4:e29.

Lee WC, Chen JL, Huang H, Leslie JH, Amitai Y, So PT, Nedivi E (2008) A dynamic zone defines interneuron remodeling in the adult neocortex. Proc Natl Acad Sci U S A 105:19968–19973.

LeVay S, Stryker MP, Shatz CJ (1978) Ocular dominance columns and their development in layer IV of the cat's visual cortex: a quantitative study. J Comp Neurol 179:223–244.

LeVay S, Wiesel TN, Hubel DH (1980) The development of ocular dominance columns in normal and visually deprived monkeys. J Comp Neurol 191:1–51.

Majewska AK, Newton JR, Sur M (2006) Remodeling of synaptic structure in sensory cortical areas in vivo. J Neurosci 26:3021–3029.

McBain CJ, Fisahn A (2001) Interneurons unbound. Nat Rev Neurosci 2:11–23.

Mountcastle VB (1997) The columnar organization of the neocortex. Brain 120:701–722.

O'Leary DD, Schlaggar BL, Tuttle R (1994) Specification of neocortical areas and thalamocortical connections. Annu Rev Neurosci 17:419–439.

Paxinos G, Franklin KBJ (2004) The mouse brain in stereotaxic coordinates, Compact 2nd Edition. Amsterdam; Boston: Elsevier Academic.

Rioult-Pedotti MS, Friedman D, Hess G, Donoghue JP (1998) Strengthen-

ing of horizontal cortical connections following skill learning. Nat Neurosci 1:230–234.

Schlaggar BL, O'Leary DD (1991) Potential of visual cortex to develop an array of functional units unique to somatosensory cortex. Science 252:1556–1560.

Sharma J, Angelucci A, Sur M (2000) Induction of visual orientation modules in auditory cortex. Nature 404:841–847.

Singer W (1996) Neurophysiology: the changing face of inhibition. Curr Biol 6:395–397.

Smith PH, Manning KA, Uhlrich DJ (2010) Evaluation of inputs to rat primary auditory cortex from the suprageniculate nucleus and extrastriate visual cortex. J Comp Neurol 518:3679–3700.

Stepanyants A, Hof PR, Chklovskii DB (2002) Geometry and structural plasticity of synaptic connectivity. Neuron 34:275–288.

Wagor E, Mangini NJ, Pearlman AL (1980) Retinotopic organization of striate and extrastriate visual cortex in the mouse. J Comp Neurol 193:187–202.

Wang Q, Burkhalter A (2007) Area map of mouse visual cortex. J Comp Neurol 502:339–357.

Xu HT, Pan F, Yang G, Gan WB (2007) Choice of cranial window type for in vivo imaging affects dendritic spine turnover in the cortex. Nat Neurosci 10:549–551.

Zuo Y, Lin A, Chang P, Gan WB (2005) Development of long-term dendritic spine stability in diverse regions of cerebral cortex. Neuron 46:181–189.